

# A new LDL-masked liposomal doxorubicin overcomes drug resistance in osteosarcoma

Elena Gazzano , Joanna Kopecka , Carolina Dimas Belisario , Costanzo Costamagna and Chiara Riganti \*

Department of Oncology, University of Torino, 10126 Torino, Italy

\*Correspondence: [chiara.riganti@unito.it](mailto:chiara.riganti@unito.it) (Chiara Riganti)

DOI: [10.31083/j.jmcm.2019.01.6161](https://doi.org/10.31083/j.jmcm.2019.01.6161)

This is an open access article under the CC BY-NC 4.0 license (<https://creativecommons.org/licenses/by-nc/4.0/>).

One of the chemotherapeutic drugs in the first-line treatment of osteosarcoma is doxorubicin (dox). However, its anticancer efficacy is limited by the overexpression of the multidrug efflux transporter P-glycoprotein (Pgp) which extrudes doxorubicin, disrupts drug accumulation and thus hinders the cytotoxic activity of dox. The drug extrusion activity of Pgp is enhanced by the presence of cholesterol within the plasma membrane. Pgp expression is up-regulated by multiple transcription factors including hypoxia inducible factor-1 $\alpha$  (HIF-1 $\alpha$ ). Decreasing Pgp expression and drug efflux activity may enhance the efficacy of doxorubicin against drug resistant osteosarcoma. To achieve this goal, we treated two human dox-sensitive cell lines (U-2OS and Saos-2), and their sublines displaying increasing Pgp levels and dox resistance, with a non-toxic dose of atorvastatin. This statin was able to decrease the biosynthesis of farnesyl pyrophosphate (FPP) and cholesterol, two key metabolites that were markedly increased in drug resistant sublines. By reducing the FPP levels, atorvastatin decreased the Ras/ERK1/2/HIF-1 $\alpha$  axis and down-regulated Pgp expression. Moreover, by decreasing cholesterol biosynthesis atorvastatin increased the levels of low density lipoprotein receptor (LDLR), that was also progressively increased in the dox-resistant sublines. Taking advantage of this findings, we treated dox-resistant osteosarcoma with atorvastatin followed by treatment with dox encapsulated in liposomes decorated with an LDLR-binding peptide, hence facilitating binding to, and endocytosis via LDLR. This treatment strategy induced high retention of dox in dox-resistant cells, reduced cell viability in vitro and displayed growth inhibition of dox-resistance in mouse xenograft model. Hence, we propose the combination of statins plus LDL-decorated liposomal dox as a novel treatment strategy for Pgp-expressing multidrug resistant osteosarcomas.

## Keywords

Osteosarcoma; doxorubicin; P-glycoprotein; atorvastatin; low density lipoprotein receptor; apoB100; liposomes

## 1. Introduction

The treatment of osteosarcoma is based on surgery and neo-adjuvant or adjuvant chemotherapy, including cisplatin,

methotrexate and doxorubicin (dox). Notwithstanding the large number of trials evaluating the efficacy of new drugs, such as targeted-therapies or immunotherapies, the patients' outcome did not improve in the last decades and chemotherapy remains the first therapeutic option [1]. Chemotherapy, however, achieves disease control in no more than 60% patients [2]. Resistance to cisplatin is often associated with the expression of the detoxifying enzyme glutathione transferase p1 [3]. Resistance to methotrexate is linked to the decreased expression of the reduced folate carrier SLC19A1, i.e. the primary influx transporter of antifolate [4, 5, 6], and/or foylpolypoly- $\gamma$ -glutamate synthetase [7], i.e. the glutamyl-transferase that retains folates within cells. Resistance to dox is due to both decreased influx and decreased efflux of the drug [8]. The main efflux transporter is the ATP binding cassette B1/P-glycoprotein (ABCB1/Pgp), encoded by *mdr1* gene [9, 10], which is a negative prognostic factor in osteosarcoma patients [11].

The optimal conformation of Pgp is maintained by a controlled amount of plasma-membrane cholesterol and phospholipids [12] that have a strong impact on Pgp drug efflux activity [13]. Cholesterol specifically binds a sterol-binding motif present within a transmembrane domain of Pgp [14]. Indeed, depleting cholesterol from the plasma membrane with methyl- $\beta$ -cyclodextrin, statins [15], zoledronic acid [16] or  $\omega$ 3-fatty acids [17], have reduced Pgp efflux activity in cells dox-resistant cells. Of note, dox-resistant colon cancer, malignant pleural mesothelioma, lung cancer, breast cancer and chronic lymphocytic leukemia cells [16, 18, 19, 20] have an enhanced biosynthesis of cholesterol and upstream metabolites as farnesyl pyrophosphate (FPP). This metabolic feature results in up-regulation of Pgp. Indeed, FPP activates Ras and the Ras/ERK1/2 axis that in turn phosphorylates and stabilizes the transcription factor Hypoxia Inducible Factor-1 $\alpha$  (HIF-1 $\alpha$ ), a strong inducer of *mdr1* gene expression [16, 21]. Interfering with this cascade has successfully reduced the Pgp levels in MDR cells [16, 18].

Statins decrease proliferation and invasion, and increase apoptosis in osteosarcoma cells, by inhibiting both the pro-survival JNK/c-Jun, RhoA-AMPK/p38-MAPK and JAK2/STAT5 pathways, and the release of matrix metalloproteinases [22, 23, 24, 25]. Statins have also shown additive cytotoxic effects with dox or cisplatin, producing an enhanced inhibition of proliferation and invasion [26]. More recently, it has been demonstrated that statins prevent the induction of the stemness phenotype and metastasis elicited by dox in drug resistant osteosarcoma cells [27].

Zoledronic acid, which also inhibits FPP biosynthesis and reduces the FPP-mediated post-translational modification of Ras, has shown chemosensitizing effects, since it synergizes with the mTOR inhibitor Everolimus and overcomes resistance to this drug [28]. These findings prompted us to explore inhibition of cholesterol synthesis as a promising strategy to enhance the efficacy of chemotherapy or targeted-therapy in osteosarcoma cells. Furthermore, how the MDR mediated by Pgp can be overcome by cholesterol-lowering agents, has never been addressed in this tumor.

In the present study we validated a new combination treatment based on atorvastatin and dox-encapsulated liposomes decorated with LDL, against Pgp-overexpressing human osteosarcoma cells in vitro as well as mouse xenografts in vivo. We demonstrate that this approach restores the cytotoxic efficacy of dox, increases drug uptake into cancer cells and markedly reduces drug efflux.

## 2. Materials and Methods

### 2.1 Chemicals

Fetal bovine serum and culture medium were from Invitrogen Life Technologies (Carlsbad, CA). Plastic ware for cell tissue cultures was from Falcon (Becton Dickinson, Franklin Lakes, NJ). The protein content in cell extracts was determined with the BCA kit from Sigma Chemical Co. (St. Louis, MO). Electrophoresis reagents were obtained from Bio-Rad Laboratories (Hercules, CA). Dox was purchased from Sigma Chemical Co. Unless otherwise specified, all the other reagents were from Sigma Chemical Co.

### 2.2 Cell lines

Human dox-sensitive osteosarcoma U-2OS and Saos-2 cell lines were purchased from ATCC (Manassas, VA). The corresponding variants with increasing resistance to dox (U-2OS/DX30, U-2OS/DX100, U-2OS/DX580, Saos-2/DX30, Saos-2/DX100, Saos-2/DX580), selected by culturing parental cells in medium containing 30, 100, 580 ng/ml dox, respectively, were generated as previously described [29]. All cell lines were authenticated by microsatellite analysis, using the PowerPlex kit (Promega Corporation, Madison, WI; last authentication: January 2019).

### 2.3 Cholesterol and FPP biosynthesis

Cells were labeled with 1  $\mu\text{Ci}/\text{mL}$  [ $^3\text{H}$ ]-acetate (3600 mCi/mmol; Amersham Bioscience, Piscataway, NJ) for 24 h. The synthesis of the radiolabeled cholesterol and FPP was determined after lipid extraction, separation by thin layer chromatography (TLC) and liquid scintillation counting [30]. Results were expressed as pmoles/mg protein, according to the relative calibration curves.

### 2.4 Immunoblotting

Cells were lysed in MLB buffer (Millipore, Burlington, MA), sonicated and centrifuged at 13,000  $\times$  g for 10 min at 4 °C. Twenty  $\mu\text{g}$  cell lysates were subjected to 4-15% SDS-PAGE and probed with the following antibodies: anti-Ras (clone RAS10, diluted 1 : 1,000; Millipore); anti-phospho-(Thr202/Tyr204, Thr185/Tyr187)-ERK1/2 (#05-797R, diluted 1 : 500; Millipore); anti-ERK1/2 (#06-182, diluted 1 : 500; Millipore); anti-HIF-1 $\alpha$  (clone 54/HIF-1 $\alpha$ , diluted 1 : 500; BD Bioscience, San Jose, CA); anti-ABC1/Pgp (clone C219, diluted 1 : 500, Millipore); anti-LDL

receptor (LDLR; clone EP1553Y, diluted 1 : 500; Abcam, Cambridge, CA); anti- $\beta$ -tubulin (clone D10, diluted 1 : 1,000, Santa Cruz Biotechnology Inc., Santa Cruz, CA), followed by the secondary peroxidase-conjugated antibodies (Bio-Rad). Proteins were detected by enhanced chemiluminescence (Bio-Rad). The amount of Ras-GTP bound fraction, taken as an index of active Ras [31], was measured by a pull-down assay, using the Raf-1-GST fusion protein, agarose beads-conjugates (Millipore), as per manufacturer's instructions. To assess HIF-1 $\alpha$  phosphorylation, the whole cell lysate was immunoprecipitated with the anti-HIF-1 $\alpha$  antibody (clone H1 $\alpha$  67, diluted 1 : 50; Santa Cruz Biotechnology Inc.), then probed for 1 h with a biotin-conjugated anti-phosphoserine antibody (Sigma Chemical Co.), followed by reaction with polymeric streptavidin-horseradish peroxidase conjugates (Sigma Chemical Co.).

### 2.5 Electrophoretic mobility shift assay (EMSA)

Nuclear proteins were extracted using the Nuclear Extract Kit (Active Motif, Rixensart, Belgium). To measure the transcriptional activity of HIF-1 $\alpha$ , EMSA was performed as previously described [32].

### 2.6 qRT-PCR

RNA was extracted and reverse-transcribed using the iScript™ cDNA Synthesis Kit (Bio-Rad Laboratories). qRT-PCR was performed using IQ™ SYBR Green Supermix (Bio-Rad Laboratories). The same cDNA preparation was used for measuring genes of interest and the housekeeping gene S14. Primer sequences were designed using qPrimerDepot software (<http://primerdepot.nci.nih.gov/>). Relative gene expression levels were calculated using Gene Expression Quantitation software (Bio-Rad Laboratories).

### 2.7 Flow cytometry analysis

ABC1/Pgp levels on cell surface were determined as previously described [33]. Samples were analyzed using Guava® easyCyte flow cytometer (Millipore) and InCyte software (Millipore). Control experiments included incubation of cells with non-immune isotypic antibody, followed by secondary antibody.

### 2.8 Cellular Dox accumulation

Dox content was determined fluorimetrically [34], using a Synergy HT Multi-Detection Microplate Reader (Bio-Tek Instruments, Winoosky, MT). The results were expressed as nmoles dox/mg protein, according to a calibration curve previously set.

### 2.9 Cytotoxicity and cell viability

The extracellular release of lactate dehydrogenase (LDH), considered an index of cell damage and necrosis, was measured as reported previously [34]. Cell viability was measured by the AT-Plite Luminescence Assay System (PerkinElmer, Waltham, MA), using the manufacturer's instructions. Results were expressed as percentage of viable cells relative to untreated cells, considered 100% viable.

### 2.10 Apo-Lipodoxorubicin production

Synthesis and characterization of the LDL-decorated liposomes loaded with dox, termed apo-Lipodox (aLD), was reported previously [15]. Briefly, anionic liposomes (COATSOME EL-01-PA, from NOF Corporation, Tokyo, Japan) were incubated with 1.5 mM dox in sterile aqueous solution, according to the

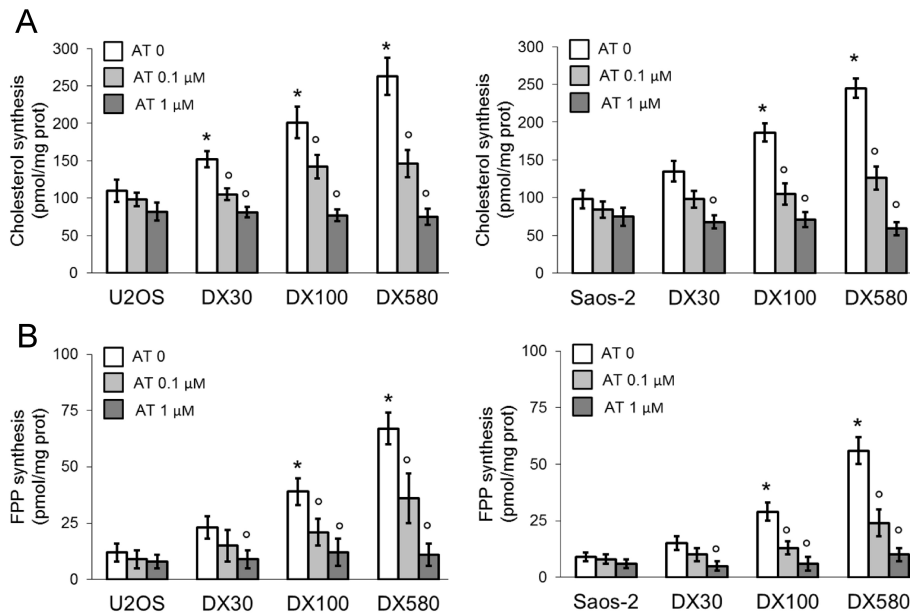


Figure 1. Atorvastatin decreases the rate of cholesterol and FPP biosynthesis in dox-resistant osteosarcoma cells. Human dox-sensitive U-2OS and Saos-2 cells and their dox-resistant sublines DX30, DX100 and DX580 were incubated for 24 h with 1  $\mu$ Ci [ $^3$ H]-acetate, in the absence (0) or presence of 0.1 and 1  $\mu$ M atorvastatin (AT), and then subjected to lipid extraction, separation by TLC. The amount of neo-synthesized cholesterol (panels A) and FPP (panels B) were determined by liquid scintillation counting, in duplicates. Data are means  $\pm$  SD (n = 3 independent experiments). \*P < 0.047 for untreated DX-cells vs. parental U-2OS or Saos-2 cells; P < 0.0023 for AT-treated cell subline vs. the corresponding untreated cell subline.

manufacturer's instructions. The residual non-encapsulated drug was removed by gel filtration using a Sephadex G-50 column. The amount of encapsulated dox was quantified fluorimetrically. The liposomes with an encapsulation efficiency >85% were collected and incubated with 2.5  $\mu$ M of a recombinant peptide from human apoB100 containing an amphipathic helix, for the insertion in the liposomes, and the LDLR binding site on the outer surface: DWLKAFYDKVAEKLKEAFRLTRKRGLKLA (the LDLR-binding site is underlined; GenScript (Piscataway, NJ)). The unbound peptide was removed by dialysis [35]. The amount of peptides incorporated was detected by the QuantiPro BCA Assay kit (Sigma Chemical Co.).

### 2.11 In vivo tumor growth

$1 \times 10^7$  U-2OS/DX580 cells, re-suspended in 100  $\mu$ l Matrigel (Sigma), were subcutaneously implanted in 6-week old female *nu/nu* Balb/C mice. Tumor volume was monitored by caliper and calculated according to the equation:  $(L \times W^2)/2$ , where L = tumor length and W = tumor width. When tumors reached the volume of 50 mm<sup>3</sup>, animals were randomized and treated as reported in the legend of Fig. 4. Tumor volumes were monitored daily by caliper and animals were euthanized with zolazepam (0.2 ml/kg) and xylazine (16 mg/kg) at day 21 after. Tumors were collected and photographed, then homogenized for 30 s at 15 Hz, using a TissueLyser II device (Qiagen, Hilden, Germany) and clarified at 12,000 x g for 5 min. Ten  $\mu$ g of proteins from tumor lysates were used for the immunoblot analysis of Pgp, LDLR and  $\beta$ -tubulin, as reported above. Animal care and experimental procedures were approved by the Bio-Ethical Committee of the Italian Ministry of Health (#122/2015-PR).

### 2.12 Statistical analysis

All data in text and figures are presented as means  $\pm$  SD. The results were analyzed by a one-way analysis of variance (ANOVA), using Statistical Package for Social Science (SPSS) software (IBM SPSS Statistics v. 19). P < 0.05 was considered statistically significant.

## 3. Results

### 3.1 Atorvastatin reduces cholesterol and FPP synthesis, and Pgp expression in dox-resistant osteosarcoma cells

Human dox-sensitive U-2OS and Saos-2 cells as well as their dox-resistant sublines DX30, DX100 and DX580, characterized by increasing levels of Pgp and consequently resistance to dox [30], were analyzed for the *de novo* biosynthesis of cholesterol (Fig. 1A) and FPP (Fig. 1B) by metabolic radiolabeling. In line with the findings obtained in other solid tumors [15, 16], in osteosarcoma cells too, the increase in dox-resistance was paralleled by an increase in the rate of cholesterol and FPP biosynthesis. This biosynthesis was however inhibited by atorvastatin, in a dose-dependent manner (Fig. 1A-B). Since 1  $\mu$ M atorvastatin decreased both cholesterol and FPP synthesis in all cell lines (Fig. 1A-B), without inducing necrotic damage after 24 h, as demonstrated by the lack of increase in the extracellular LDH (Fig. S1A-B), and without decreasing cell viability after 48 h (Fig. S1B), we used this concentration for all the following experiments.

Dox-resistant sublines of U-2OS cells displayed a higher level of GTP-bound Ras, i.e. the active form of the protein (Fig. 2A), likely as a consequence of the high supply of FPP [31]. The levels of active phosphorylated ERK1/2, a downstream effector of Ras,

were also increased in the dox-resistant sublines. Phosphorylated HIF-1 $\alpha$ , a target of ERK1/2 kinase, was detected in dox-resistant osteosarcoma sublines (Fig. 2A). In these cells, HIF-1 $\alpha$  was bound to its consensus sequence on DNA (i.e. hypoxia response element; Fig. 2B), suggesting that HIF-1 $\alpha$  was transcriptional active. In parallel, the mRNA levels of *mdr1*, a target gene of HIF-1 $\alpha$  [21], were increased in dox-resistant sublines (Fig. 2C). The levels of Pgp in whole cell lysates (Fig. 2D) and on the cell surface (Fig. 2E) were progressively increased in the U-2OS/DX30, U-2OS/DX100 and U-2OS/DX580 sublines.

Atorvastatin, which did not significantly reduce FPP biosynthesis in U-2OS cells (Fig. 1B), did not change the activation of Ras/ERK1/2/HIF-1 $\alpha$  axis, nor the amount of Pgp (Fig. 2A-E) in sensitive cells. In contrast, in dox-resistant clones, where the statin induced a stronger decrease in FPP levels (Fig. 1B), atorvastatin potently repressed the activation of Ras/ERK1/2 (Fig. 2A), the phosphorylation and the transcriptional activity of HIF-1 $\alpha$  (Fig. 2A-B), the levels of *mdr1* mRNA (Fig. 2C) and Pgp protein (Fig. 2D-E).

### 3.2 The combination of atorvastatin and dox loaded liposomes decorated with an LDLR binding peptide reverses drug resistance in refractory osteosarcoma.

We previously observed that dox-resistant cells have increased levels of LDLR [15]. Accordingly, dox-resistant osteosarcoma sublines progressively increased the expression of LDLR (Fig. 3A) and the amount of LDLR on cell surface (Fig. 3B), in parallel with the increase of dox-resistance. In mammalian cells, the physiological response to the decrease in intracellular cholesterol is the increase of LDLR [36]. In line with this metabolic response, osteosarcoma cells treated with atorvastatin, which reduced intracellular cholesterol (Fig. 1A), increased the expression of LDLR (Fig. 3A-B). The increase in LDLR was higher in most dox-resistant sublines, where the effects of atorvastatin on cholesterol biosynthesis were stronger.

Taking advantage of this phenotype, we designed a treatment strategy based on a 24 h incubation with atorvastatin, to increase LDLR, followed by a 24 h incubation with liposomal dox decorated with the recombinant apoB100-derived peptide containing the LDLR binding site (Fig. 3C). When used alone, these liposomes (aLD) were slightly more accumulated in all the dox-resistant sublines than free dox (Fig. 3D; Fig. S2A). This increase, however, did not reduce cell viability in the sublines resistant to dox (Fig. 3E; Fig. S2B). Remarkably, pre-treatment with atorvastatin followed by aLD significantly enhanced the intracellular retention of dox (Fig. 3D; Fig. S2A) and reduced the viability of cells in all dox-resistant sublines (Fig. 3E; Fig. S2B).

To validate the efficacy of our treatment scheme in a preclinical model of resistant osteosarcoma, we subcutaneously implanted U-2OS/DX580 cells in adult *nu/nu* Balb/c mice. Expectedly, dox did not reduce the growth of tumors that turned out to be resistant to Caelyxto<sup>®</sup>, the clinically-approved formulation of liposomal dox (Fig. 4A). aLD alone slightly reduced tumor growth, but the maximal efficacy was achieved by the treatment with atorvastatin, at a dose ineffective in decreasing tumor growth, followed by aLD after 24 h (Fig. 4A). The analysis of tumor extracts demonstrated that atorvastatin-treated mice had lower Pgp but higher LDLR levels (Fig. 4B), recapitulating the phenotype observed *in vitro*.

## 4. Discussion

In the current study, we evaluated a new pre-clinical strategy in an attempt to overcome dox-resistance mediated by Pgp in osteosarcoma. As already observed in several dox-resistant tumors [16], in osteosarcoma cell lines too, the rate of cholesterol biosynthesis was increased upon increase in Pgp expression and acquired dox resistance. Cholesterol and its upstream metabolites, including FPP, are indeed critical contributors to Pgp expression and efflux activity. First, cholesterol plasma membrane cholesterol maintains an optimal conformation of Pgp [13, 14]. Second, the amount of FPP is crucial for the activation of the Ras/ERK1/2/HIF-1 $\alpha$  axis [16, 18]. In line with the higher rate of FPP biosynthesis, the activity of the Ras/ERK1/2/HIF-1 $\alpha$  cascade and the transcriptional activity of HIF-1 $\alpha$  were progressively increased upon gradual acquisition of dox resistance in osteosarcoma cells. Accordingly, *mdr1* mRNA and Pgp protein level were significantly elevated.

In order to reduce both the expression and drug efflux activity of Pgp, we used atorvastatin, a potent inhibitor of 3- $\beta$ -hydroxy-3- $\beta$ -methyl-glutaryl coenzyme A reductase, the rate-limiting enzyme in cholesterol biosynthesis. By inhibiting the pathway at this step, we obtained a simultaneous decrease in the levels of both FPP and cholesterol. The decrease was negligible in sensitive cells and proportionally higher in most dox-resistant sublines. Indeed, higher the basal rate of biosynthesis, the stronger was the effect of atorvastatin in reducing the rate of FPP and cholesterol biosynthesis; this resulted in decreased activation of Ras/ERK1/2/HIF-1 $\alpha$  axis and Pgp levels. The decrease in cell surface Pgp, i.e. the active form of Pgp, was due to a decreased transcription, as demonstrated by the reduction of *mdr1* mRNA.

Atorvastatin was previously found to be a pro-apoptotic agent in osteosarcoma cells when used at a 10  $\mu$ M concentration [22], a finding that was also confirmed in U-2OS and Saos-2 cells. To avoid any bias due to a direct cytotoxic effect of the statin and to investigate the effect of the statin as a pure chemosensitizing agent, we used the drug at a 1  $\mu$ M concentration as the most effective concentration that reduced cholesterol and FPP synthesis, without inducing cell toxicity.

As a consequence of the effective decrease in cholesterol synthesis, atorvastatin-treated cells increased the expression of LDLR. Of note, chemoresistant cells have a higher basal level of LDLR [15], likely because they have an enormous demand for cholesterol of either endogenous or exogenous origin to maintain proper homeostasis of their plasma membrane [17]. Osteosarcoma cells are no exception to this behavior drug-sensitive U-2OS cells had very low levels of LDLR, while their dox-resistant sublines progressively increased the expression of this receptor. In line with the higher decrease in cholesterol biosynthesis exerted by atorvastatin, LDLR was reduced by atorvastatin in dox-resistant cells more than in sensitive ones.

Since dox-resistance is not only due to an increased drug efflux, but also due to a decreased drug uptake [9], we designed a treatment strategy that increased the uptake of dox via LDLR and decreased its efflux via Pgp. We pre-treated cells with atorvastatin, in order to increase surface LDLR levels, and then we administered dox in a liposomal formulation decorated with the LDLR-binding peptide derived from apoB100. In dox-resistant colon cancer cells,

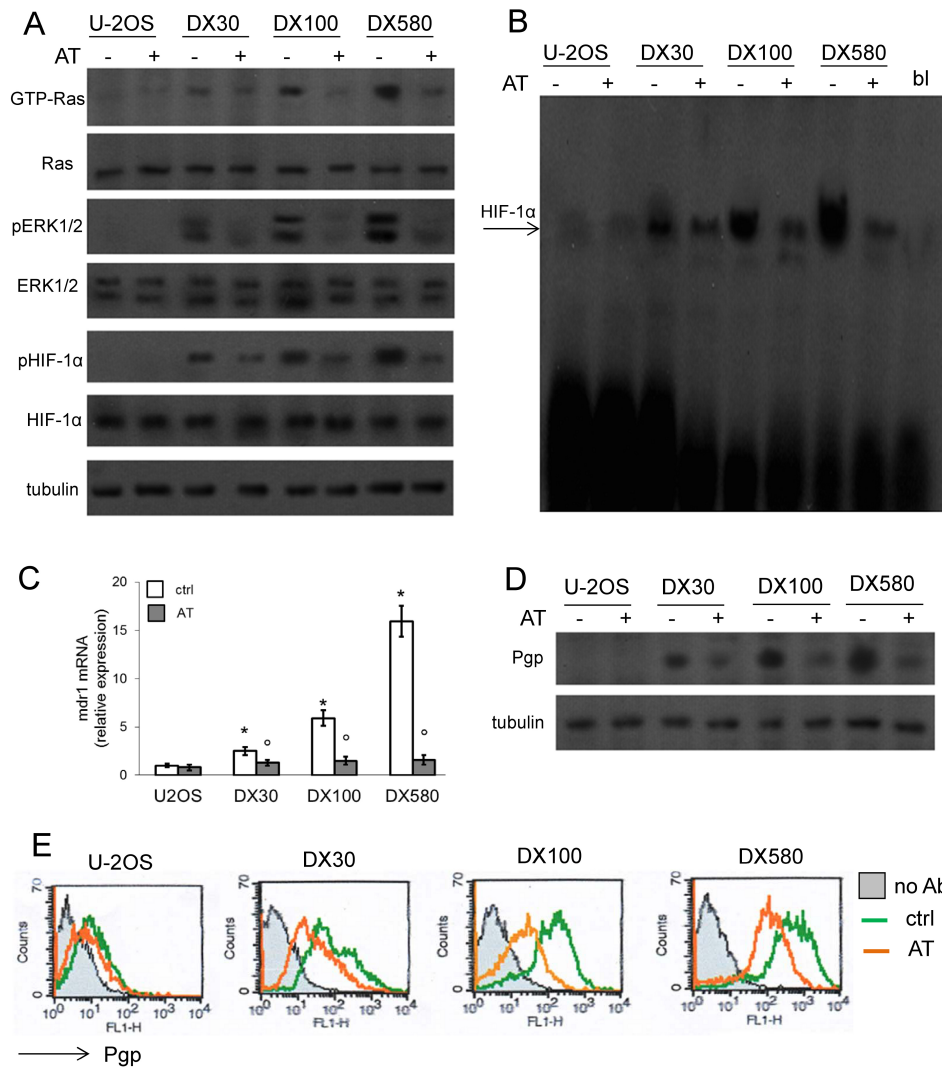


Figure 2. Atorvastatin down-regulates the expression of P-glycoprotein in doxorubicin-resistant osteosarcoma cells. Human dox-sensitive U-2OS cells and their resistant sublines DX30, DX100 and DX580 were incubated 24 h in the absence (-, ctrl) or presence (+) of 1  $\mu$ M atorvastatin (AT). A. Expression levels of the indicated proteins in whole cell lysates as determined by Western blot analysis. The  $\beta$ -tubulin expression was used as control for equal protein loading. The figure is representative of 3 independent experiments. B. Binding of nuclear HIF-1 $\alpha$  to its DNA consensus binding sequence, was measured by EMSA. The figure is representative of 3 independent experiments. Bl: blank. C. *mdr1* mRNA levels determined by qRT-PCR, in triplicates. Data are means  $\pm$  SD (n = 3 independent experiments). \* $P$  < 0.001 for untreated DX-cells vs. parental U-2OS cells; <sup>o</sup> $P$  < 0.018 for AT-treated cell variant vs. the corresponding untreated cell variant. D. Pgp levels in whole cell lysates by immunoblotting. The  $\beta$ -tubulin expression was used as a control of equal protein loading. The figure is representative of 3 independent experiments. E. Cell surface Pgp levels determined by flow cytometry, in duplicates. No Ab: cells incubated with non-immune isotypic antibody. Histograms are representative of 3 independent experiments.

this treatment favored the entry of LDL-decorated liposomal dox via a receptor-mediated endocytosis and achieved a high intracellular drug delivery [15]. In dox-resistant osteosarcoma cells, the sequential treatment of atorvastatin plus LDL-decorated liposomal dox significantly increased the amount of intracellular dox -- that attained the same levels obtained in sensitive cells -- and the consequent cytotoxicity. These effects were not cell-specific, since they were observed in two different osteosarcoma cell lines.

Liposomal dox has been widely exploited as a new strategy to improve the efficacy of the drug against resistant osteosarcoma, using targeted liposomes able to increase the drug delivery into

osteosarcoma cells [37, 38, 39]. Our approach is innovative because we adopted a Trojan horse strategy that increased the drug uptake and reduced the drug efflux.

We finally validated our novel treatment strategy in dox-resistant osteosarcoma xenografts, that were completely resistant to dox. Atorvastatin was given at a concentration equivalent to the dose administered to hypercholesterolemic patients, i.e. 40 mg/day [30]. At this dosage, the statin had no anti-tumor effect. Since the half-life of atorvastatin is 14 h and the half-life of its active metabolite ranges between 20 and 30 h, it is reasonable to think that upon atorvastatin was able to lower cholesterol synthesis,

increase LDLR and decrease Pgp. Indeed, the sequential administration of atorvastatin followed by LDL-decorated liposomal dox after 24 h was very effective in reducing tumor growth. The analysis of tumor extracts confirmed that in this group, there was a maximal increase in both LDLR and a maximal decrease in Pgp, providing the rationale explanation of the high anti-tumor efficacy of our combined treatment.

Notably, our approach was superior to Caelyx<sup>®</sup>, the FDA-approved liposomal formulation of dox that prevented the onset of dox cardiotoxicity [40, 41] but did not improve dox efficacy against Pgp-expressing tumors [42, 43], including osteosarcoma [36].

## 5. Conclusions

We propose an innovative two-steps treatment based on the sequential administration of atorvastatin and LDL-masked liposomal dox, that was effective against dox-resistant/Pgp-expressing osteosarcoma. By exploiting an Achilles' heel of dox-resistant cells - i.e. the high sensitivity to the metabolic effect of statins - we increased dox uptake, taking advantage from the high expression of LDLR and decreased dox efflux, taking advantage from the decreased expression of Pgp. Our strategy may be considered as a potential treatment for Pgp-overexpressing osteosarcomas, characterized by strong resistance to dox and consequently poor prognosis.

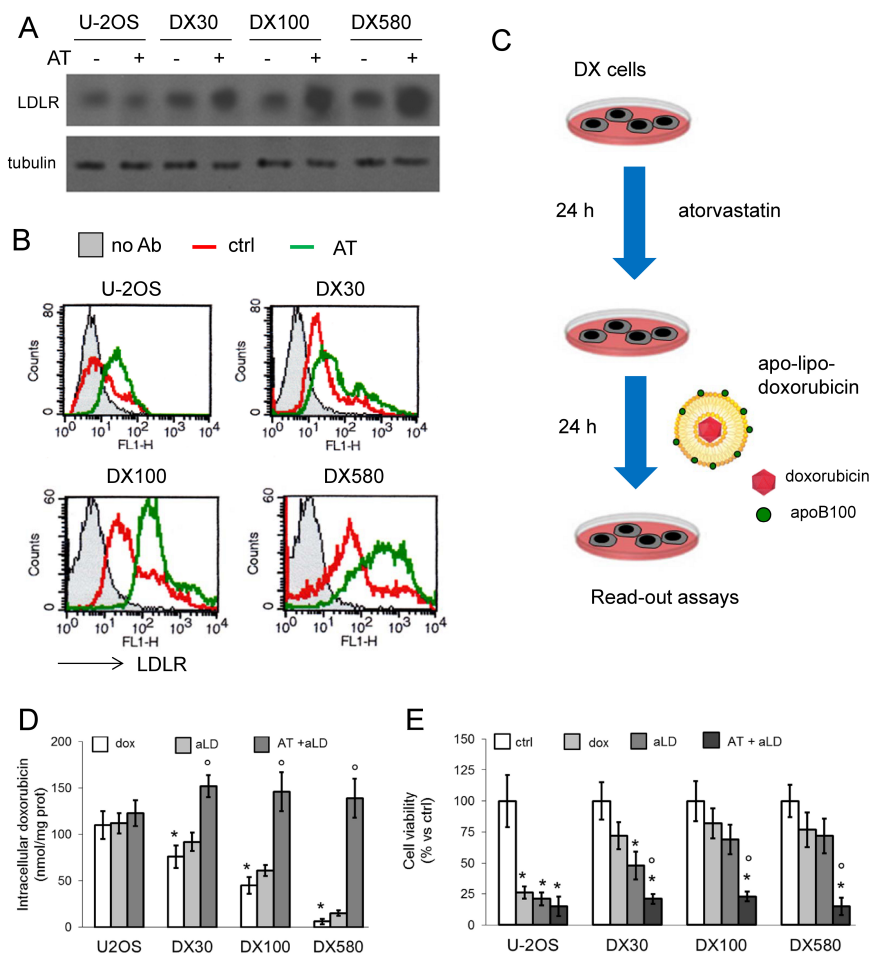
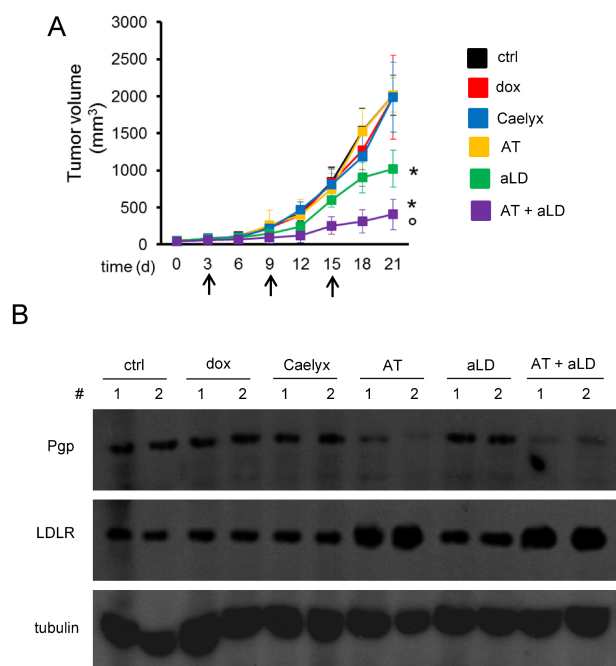


Figure 3. The sequential treatment with atorvastatin and LDL-decorated liposomal dox overcomes drug resistance in osteosarcoma cells. A. Human dox-sensitive U-2OS cells and their resistant sublines DX30, DX100 and DX580 were incubated 24 h in the absence (-, ctrl) or presence (+) of 1  $\mu$ M atorvastatin (AT). Cells were lysed and analyzed for the expression of low density lipoprotein receptor (LDLR) by immunoblotting. The  $\beta$ -tubulin expression was used as an internal control for equal protein loading. The figure is representative of 3 independent experiments. B. Cell surface LDLR levels were measured by flow cytometry, in duplicates. No Ab: cells incubated with non-immune isotypic antibody. Histograms are representative of 3 independent experiments. C. Experimental scheme of the sequential treatment with atorvastatin and LDL-decorated dox-loaded liposomes. Cells were incubated for 24 h with 1  $\mu$ M AT, then with LDL-decorated liposomal dox (apo-Lipodox, aLD) containing 5  $\mu$ M dox for an additional 24 h. Cells were incubated for 24 h with 5  $\mu$ M dox, 24 h with 5  $\mu$ M aLD, 24 h with 1  $\mu$ M AT followed by 24 h with 5  $\mu$ M aLD. Intracellular dox accumulation was measured fluorimetrically, in duplicates. Data are means  $\pm$  SD (n = 3 independent experiments). \* $P$  < 0.044 for untreated DX-cells vs. parental U-2OS cells;  $^{\circ}P$  < 0.001 for AT+aLD-treated cells vs. the corresponding dox-treated cells. D. Cells treated as in C, were grown for additional 24 h. Percentage of viable cells, measured by a chemiluminescence-based assay, in quadruplicates. Data are means  $\pm$  SD (n = 3 independent experiments). \* $P$  < 0.001 for treated vs. untreated (ctrl) cells;  $^{\circ}P$  < 0.001 for AT+aLD-treated cells vs. the corresponding dox-treated cells.



**Figure 4.** The sequential treatment with atorvastatin and LDL-masked liposomal doxorubicin reduces the growth of drug-resistant osteosarcoma. U-2OS/DX580 cells were subcutaneously implanted in 6-week old female *nu/nu* Balb/C mice. When tumors reached a volume of 50 mm<sup>3</sup>, animals were randomized in 6 groups (n = 6 mice/group) and treated at day 3, 9, and 15 after randomization (indicated by the arrows in the figure) as it follows: 1) control (ctrl) group, treated with 200  $\mu$ l sterile physiological solution, intravenously (i.v.); 2) dox (dox) group, treated with 200  $\mu$ l sterile physiological solution containing 5 mg/kg dox, i.v.; 3) Caelyx<sup>®</sup> group, treated with 200  $\mu$ l sterile solution of Caelyx<sup>®</sup>, equivalent to 5 mg/kg dox, i.v.; 4) atorvastatin (AT) group, treated with 200  $\mu$ l of saline solution containing 12  $\mu$ g atorvastatin, by oral gavage; 5) LDL-decorated liposomal dox (apo-Lipodoxorubicin, aLD), treated with 200  $\mu$ l sterile physiological solution containing 5 mg/kg dox, i.v.; 6) AT + aLD group, treated with 12  $\mu$ g atorvastatin, by oral gavage, followed by 5 mg/kg dox, i.v., 24 h after the statin. A. Tumor growth was monitored daily by caliper measurement. Data are presented as means  $\pm$  SD. \* $P$  < 0.0026 for aLD vs all other treatment groups (day 21); \* $P$  < 0.00 for AT+aLD vs all other treatment groups (days 15-21);  $\circ P$  < 0.001 for AT+aLD vs aLD group (days: 15-21).

## Abbreviations

Dox: doxorubicin; ABCB1/Pgp: ATP binding cassette B1/P-glycoprotein; FPP: farnesyl pyrophosphate; HIF-1 $\alpha$ : Hypoxia Inducible Factor-1 $\alpha$ ; LDL: low density lipoprotein; TLC: thin layer chromatography; LDLR: LDL receptor; EMSA: electrophoretic mobility shift assay; LDH: lactate dehydrogenase; aLD: apo-Lipodoxorubicin; ANOVA: analysis of variance; SPSS: Statistical Package for Social Science; i.v. : intravenous.

## Authors' contributions

EG and CC performed the *in vitro* experiments; JK performed the assays in xenograft models; CDB produced the liposomal formulations; EG, JK and CDB analyzed the data; CR supervised the

study and wrote the manuscript. All authors contributed to editorial changes in the manuscript. All authors read and approved the final manuscript.

## Acknowledgment

Funding support from the Associazione Italiana per la Ricerca sul Cancro (AIRC; IG21408), the Italian Ministry of University and Research (Future in Research 2012; RBFR12SOQ1) and the Cost Action (CA17104) are greatly appreciated (CR).

## Conflict of Interest

The authors declare no competing interests.

## References

- [1] Saraf AJ, Fenger JM, Roberts RD. Osteosarcoma: Accelerating progress makes for a hopeful future. *Front Oncol*, 2018; 8: e4.
- [2] Hattinger CM, Fanelli M, Tavanti E, Vella S, Riganti C, Picci P, *et al.* Doxorubicin-resistant osteosarcoma: novel therapeutic approaches in sight? *Future Onco*, 2017; 13(8): 673-677.
- [3] Pasello M, Michelacci F, Scionti I, Hattinger CM, Zuntini M, Caccuri AM, *et al.* Overcoming glutathione S-transferase P1-related cisplatin resistance in osteosarcoma. *Cancer Res*, 2008; 68(16): 6661-6668.
- [4] Ifergan I, Meller I, Issakov J, Assaraf YG. Reduced folate carrier protein expression in osteosarcoma: implications for the prediction of tumor chemosensitivity. *Cancer*, 2003; 98(9): 1958-1966.
- [5] Sowers R, Wenzel BD, Richardson C, Meyers PA, Healey JH, Levy AS, Gorlick R. Impairment of methotrexate transport is common in osteosarcoma tumor samples. *Sarcoma*, 2011; 834170.
- [6] Assaraf, YG. Molecular basis of antifolate resistance. *Cancer Metastasis Rev*, 2007; 26: 153-181.
- [7] Raz S, Stark M, Assaraf Y. Folylpolypoly- $\gamma$ -glutamase synthetase: A key determinant of folate homeostasis and antifolate resistance in cancer. *Drug Resist Update*, 2016; 28: 43-64.
- [8] He H, Ni J, Huang J. Molecular mechanisms of chemoresistance in osteosarcoma. *Oncol Lett*, 2014, 7(5): 1352-1362.
- [9] Gottesman MM, Fojo T, Bates SE. Multidrug resistance in cancer: role of ATP-dependent transporters. *Nat Rev Cancer*, 2002; 2(1): 48-58.
- [10] Li W, Zhang H, Assaraf YG, Zhao K, Xu X, Xie J, Yang DH, Chen ZS. Overcoming ABC transporter-mediated multidrug resistance: Molecular mechanisms and novel therapeutic drug strategies. *Drug Resist Update*, 2016; 27, 14-29.
- [11] Serra M, Scotlandi K, Reverter-Branchat G, Ferrari S, Manara MC, Benini S, *et al.* Value of P-glycoprotein and clinicopathologic factors as the basis for new treatment strategies in high-grade osteosarcoma of the extremities. *J Clin Oncol*, 2003; 21(3): 536-542.
- [12] Domicveica L, Koldsø H, Biggin PC. Multiscale molecular dynamics simulations of lipid interactions with P-glycoprotein in a complex membrane. *J Mol Graph Model*, 2018; 80: 147-156.
- [13] Alam A, Kowal J, Broude E, Roninson I, Locher KP. Structural insight into substrate and inhibitor discrimination by human P-glycoprotein. *Science*, 2019; 363(6428): 753-756.
- [14] Clay AT, Lu P, Sharom FJ. Interaction of the P-Glycoprotein Multidrug Transporter with Sterols. *Biochemistry*, 2015; 54(43): 6586-6597.
- [15] Kopeccka J, Campia I, Olivero P, Pescarmona G, Ghigo D, Bosia A, *et al.* A LDL-masked liposomal-doxorubicin reverses drug resistance in human cancer cells. *J Control Rel*, 2011; 149(2): 196-205.

- [16] Riganti C, Castella B, Kopecka J, Campia I, Coscia M, Pescarmona G, *et al.* Zoledronic Acid Restores Doxorubicin Chemosensitivity and Immunogenic Cell Death in Multidrug-Resistant Human Cancer Cells. *PLoS ONE*, 2013; 8(4): e60975.
- [17] Gelsomino G, Corsetto PA, Campia I, Montorfano G, Kopecka J, Castella B, *et al.* Omega 3 fatty acids chemosensitize multidrug resistant colon cancer cells by down-regulating cholesterol synthesis and altering detergent resistant membranes composition. *Mol Cancer*, 2013; 12: e137.
- [18] Kopecka J, Porto S, Lusa S, Gazzano E, Salzano G, Giordano A, *et al.* Self-assembling nanoparticles encapsulating zoledronic acid revert multidrug resistance in cancer cells. *Oncotarget*, 2015; 6(31): 31461-31478.
- [19] Kopecka J, Porto S, Lusa S, Gazzano E, Salzano G, Pinzón-Daza ML, *et al.* Zoledronic acid-encapsulating self-assembling nanoparticles and doxorubicin: a combinatorial approach to overcome simultaneously chemoresistance and immunoresistance in breast tumors. *Oncotarget*, 2016; 7(15): 20753-20772.
- [20] Rigoni M, Riganti C, Vitale C, Griggio V, Campia I, Robino M, *et al.* Simvastatin and downstream inhibitors circumvent constitutive and stromal cell-induced resistance to doxorubicin in IGHV unmutated CLL cells. *Oncotarget*, 2015; 6(30): 29833-29846.
- [21] Kopecka J, Campia I, Jacobs A, Frei AP, Ghigo D, Wollscheid B, *et al.* Carbonic anhydrase XII is a new therapeutic target to overcome chemoresistance in cancer cells. *Oncotarget*, 2015; 6(9): 6776-6793.
- [22] Fromigué O, Hamidouche Z, Marie PJ. Blockade of the RhoA-JNK-c-Jun-MMP2 cascade by atorvastatin reduces osteosarcoma cell invasion. *J Biol Chem*, 2008; 283(45): 30549-30556.
- [23] Sandoval-Usme MC, Umaña-Pérez A, Guerra B, Hernández-Perera O, García-Castellano JM, Fernández-Pérez L, *et al.* Simvastatin impairs growth hormone-activated signal transducer and activator of transcription (STAT) signaling pathway in UMR-106 osteosarcoma cells. *PLoS One*, 2014; 9(1): e87769.
- [24] Kamel WA, Sugihara E, Nobusue H, Yamaguchi-Iwai S, Onishi N, Maki K, *et al.* Simvastatin-induced apoptosis in osteosarcoma cells: A key role of RhoA-AMPK/p38 MAPK signaling in antitumor activity. *Mol Cancer Ther*; 2017; 16(1): 182-192.
- [25] Kany S, Woschek M, Kneip N, Sturm R, Kalbitz M, Hanschen M, *et al.* Simvastatin exerts anticancer effects in osteosarcoma cell lines via geranylgeranylation and c-Jun activation. *Int J Oncol*, 2018; 52(4): 1285-1294.
- [26] Fromigué O, Hamidouche Z, Marie PJ. Statin-induced inhibition of 3-hydroxy-3-methyl glutaryl coenzyme a reductase sensitizes human osteosarcoma cells to anticancer drugs. *J Pharmacol Exp Ther*, 2008; 325(2): 595-600.
- [27] Li Y, Xian M, Yang B, Ying M, He Q. Inhibition of KLF4 by statins reverses adriamycin-induced metastasis and cancer stemness in osteosarcoma cells. *Stem Cell Rep*, 2017; 8(6): 1617-1629.
- [28] Moriceau G, Ory B, Mitrofan L, Riganti C, Blanchard F, Brion R, *et al.* Zoledronic acid potentiates mTOR inhibition and abolishes the resistance of osteosarcoma cells to RAD001 (Everolimus): pivotal role of the prenylation process. *Cancer Res*, 2010; 70(24): 10329-10339.
- [29] Serra M, Scotlandi K, Manara MC, Maurici D, Lollini PL, De Giovanni C, *et al.* Establishment and characterization of multidrug-resistant human osteosarcoma cell lines. *Anticancer Res*, 1993; 13(2): 323-329.
- [30] Riganti C, Pinto H, Bolli E, Belisario DC, Calogero RA, Bosia A, *et al.* Atorvastatin modulates anti-proliferative and pro-proliferative signals in Her2/neu-positive mammary cancer. *Biochem Pharmacol*, 2011; 82(9): 1079-1089.
- [31] Swanson KM, Hohl RJ. Anti-cancer therapy: targeting the mevalonate pathway. *Curr Cancer Drug Targets*, 2006; 6(1): 15-37.
- [32] Riganti C, Doublier S, Aldieri E, Orecchia S, Betta PG, Gazzano E, *et al.* Asbestos induces doxorubicin resistance in MM98 mesothelioma cells via HIF-1alpha. *Eur Respir J*, 2008; 32(2): 443-451.
- [33] Buondonno I, Gazzano E, Jean SR, Audrito V, Kopecka J, Fanelli M. Mitochondria-targeted doxorubicin: A new therapeutic strategy against doxorubicin-resistant osteosarcoma. *Mol Cancer Ther*, 2016; 15(11): 2640-2652.
- [34] Riganti C, Miraglia E, Viarisio D, Costamagna C, Pescarmona G, Ghigo, D, *et al.* Nitric oxide reverts the resistance to doxorubicin in human colon cancer cells by inhibiting the drug efflux. *Cancer Res*, 2005; 65: 516-525.
- [35] Nikanjam M, Blakely EA, Bjornstad KA, Shu X, Budinger TF, Forte TM. Synthetic nano-low density lipoprotein as targeted drug delivery vehicle for glioblastoma multiforme. *Int J Pharm*, 2007; 328(1): 86-94.
- [36] van de Sluis B, Wijers M, Herz J. News on the molecular regulation and function of hepatic low-density lipoprotein receptor and LDLR-related protein 1. *Curr Opin Lipidol*, 2017; 28(3): 241-247.
- [37] Federman N, Chan J, Nagy JO, Landaw EM, McCabe K, Wu AM, *et al.* Enhanced growth inhibition of osteosarcoma by cytotoxic polymerized liposomal nanoparticles targeting the alcam cell surface receptor. *Sarcoma*, 2012; 2012: e126906.
- [38] Haghirsadsat F, Amoabediny G, Naderinezhad S, Nazmi K, De Boer JP, Zandieh-Doulabi B, *et al.* EphA2 Targeted doxorubicin-nanoliposomes for osteosarcoma treatment. *Pharm. Res*, 2017; 34(12): 2891-2900.
- [39] Haghirsadsat F, Amoabediny G, Naderinezhad S, Zandieh-Doulabi B, Forouzanfar T, Helder MN. Codelivery of doxorubicin and JIP1 siRNA with novel EphA2-targeted PEGylated cationic nanoliposomes to overcome osteosarcoma multidrug resistance. *Int J Nanomedicine*, 2018; 13: 3853-3866.
- [40] Skubitiz KM. Phase II trial of pegylated-liposomal doxorubicin (Doxil) in sarcoma. *Cancer Invest*, 2003, 21(2): 167-176.
- [41] De Sanctis R, Bertuzzi A, Basso U, Comandone A, Marchetti S, Marzari A, *et al.* Non-pegylated liposomal doxorubicin plus ifosfamide in metastatic soft tissue sarcoma: results from a phase-II trial. *Anticancer Res*, 2015; 35(1): 543-547.
- [42] Gabizon A, Patil Y, La-Beck NM. New insights and evolving role of Pegylated liposomal doxorubicin in cancer therapy. *Drug Resist Update*, 2016; 29: 90-106.
- [43] Gazzano E, Rolando B, Chegaev K, Salaroglio IC, Kopecka J, Pedrini I, *et al.* Folate-targeted liposomal nitrooxy-doxorubicin: an effective tool against P-glycoprotein-positive and folate receptor-positive tumors. *J Control Rel*, 2018; 270: 37-52.

## Supplemental material

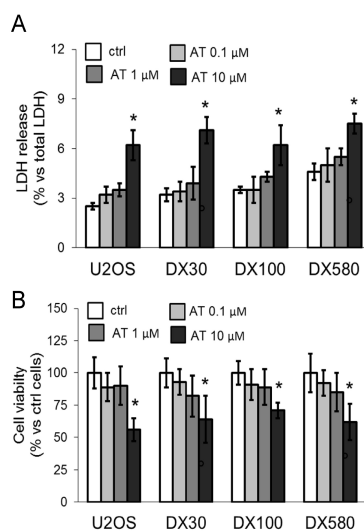


Figure S1. Dose-dependent toxicity of atorvastatin. Human dox-sensitive U-2OS cells and their resistant sublines DX30, DX100 and DX580 were grown in the absence (ctrl) or presence of 0.1, 1 or 10  $\mu\text{M}$  atorvastatin (AT). A. Extracellular LDH activity, measured spectrophotometrically after a 24 h-incubation, in duplicates. Data are means  $\pm$  SD ( $n = 3$  independent experiments).  $*P < 0.001$  for AT-treated cells vs. untreated (ctrl) cells. B. Percentage of viable cells, measured by a chemiluminescence-based assay after a 48 h-incubation, in quadruplicates. Data are means  $\pm$  SD ( $n = 3$  independent experiments).  $*P < 0.024$  for AT-treated cells vs. untreated (ctrl) cells.

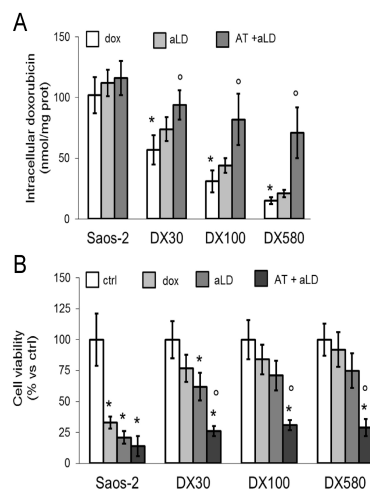


Figure S2. Effects of the sequential treatment with atorvastatin and LDL-masked liposomal doxorubicin in Saos-2 cells and in their resistant variants. A. Human dox-sensitive Saos-2 cells and their resistant sublines DX30, DX100 and DX580 were incubated 24 h in fresh medium (ctrl) or in medium containing 5  $\mu\text{M}$  doxorubicin (dox), LDL-masked liposomal doxorubicin (apo-Lipodoxorubicin, aLD) containing 5  $\mu\text{M}$  dox, 1  $\mu\text{M}$  atorvastatin (AT) for 24 h followed by 5  $\mu\text{M}$  aLD for further 24 h. Intracellular doxorubicin accumulation was measured fluorimetrically, in duplicates. Data are means  $\pm$  SD ( $n = 3$  independent experiments).  $*P < 0.0015$  for untreated DX-cells vs. parental U-2OS cells;  $^{\circ}P < 0.013$  for AT + aLD-treated cells vs. the corresponding dox-treated cells. B. Cells were incubated as in A and grown for additional 24 h. Percentage of viable cells, measured by a chemiluminescence-based assay, in quadruplicates. Data are means  $\pm$  SD ( $n = 3$  independent experiments).  $*P < 0.031$  for treated vs. untreated (ctrl) cells;  $^{\circ}P < 0.001$  for AT + aLD-treated cells vs. the corresponding dox-treated cells.